Hindawi
Advances in Civil Engineering
Volume 2020, Article ID 9670704, 10 pages
https://doi.org/10.1155/2020/9670704

Research Article

Numerical Analysis of Dead Load Shear Force Distribution in Webs of Multicell Inclined Web Box-Girder Bridge

Xingwei Xue,[1] Meizhong Wu,[1] Zhengwei Li,[2] and Peng Zhou[1]

[1]*School of Traffic Engineering, Shenyang Jianzhu University, Shenyang, Liaoning 110168, China*
[2]*Guangzhou Communications Investment Group Co., Ltd., Guangzhou, Guangdong 510000, China*

Correspondence should be addressed to Peng Zhou; zhoupeng@sjzu.edu.cn

Received 7 February 2020; Revised 28 July 2020; Accepted 17 August 2020; Published 11 September 2020

Academic Editor: Melina Bosco

Moment and shear load distribution are important in bridge design. Most existing studies have focused on the distribution of girders under vehicle loading, neglecting the dead load distribution between the webs of multicell box-girders. Through the "Sum of Local Internal Forces" function, the shear force of each web in the multicell box-girder 3D finite element model was extracted and analysed using the dead load shear force distribution factor. The research parameters include the slope of the web, support condition, and cell number with respect to the dead load shear force distribution factor. The results indicate that the dead load shear distribution in the webs of multicell box-girders is uneven. The outermost inclined web bears a shear force greater than the average shear force, which must be considered in bridge design.

1. Introduction

Inclined web box-girder bridges are common in cities. A box-girder bridge with inclined webs can increase the height of the cantilever, while reducing the bridge weight and improving aesthetics. However, the inclined web complicates the box-girder mechanics. Shear force distribution in the webs of multicell inclined web box-girder bridges under dead load is being increasingly discussed.

The concrete box section exhibits good bending and torsion resistance and has become the preferred bridge structure for large- and medium-span concrete bridges. Several researchers have conducted studies on concrete box-girder bridges [1–5].

Moment and shear load distributions are important for bridge design live-load distribution factors. Song et al. [6] investigated the live-load distribution characteristics of box-girder bridges and the limits imposed by the load and resistance factor design specifications using 3D models. The results indicated that the current load and resistance factor design distribution formulas generally provide a conservative estimate of the design bending moment and shear force. Suksawang et al. [7] developed a simplified live-load shear distribution factor for steel and prestressed concrete I-girder bridges. The results showed that the proposed equations correlate closely with finite element models based on actual bridges. Dymond [8] investigated the accuracy of existing shear distribution factors, which are used to estimate the effects of the bridge system live-load on individual girders. Different shear distribution coefficient analysis methods were recommended for calculation, with a screening tool ratio of 1.5 as the limit. Choi et al. [9] conducted an extensive parametric study to determine the maximum stress, deflection, and moment distribution factors for two-span multicell box-girder bridges based on a finite element analysis of 120 representative numerical model bridges. The results indicated that the span length, number of lanes, and number of boxes are the most important parameters affecting the load distribution factors of multicell box-girder bridges.

Most studies have focused on the distribution of girders under vehicle loading. To a large extent, researchers and designers believe that the dead load is evenly distributed between the different webs of a multicell girder. Xue [10] studied the shear force distribution caused by dead load and found that the support condition and cell number of the box

have a significant impact on the shear distribution between the webs of multicell girders, and the variation in the web thickness has little effect on the distribution. Under certain circumstances, the shear force carried by the outermost web is 1.65 times the average shear force, which indicates that the difference in the shear force distribution caused by dead load in each web cannot be neglected.

In this study, the webs are analysed according to different web slopes, cell numbers, and support conditions. The total stress-strain model, which has many practical applications [10, 11] in analysing concrete structures, uses nonlinear three-dimensional finite element analysis to study the shear redistribution of cracked webs.

2. Modelling and Web Shear Force Extraction

2.1. Modelling. The basic parameters of the simply supported box-girder in this study are span (30 m), beam height (1.8 m), top and bottom plate thickness (25 cm), middle segment length (13.6 m), web-widening segment length (4.0 m), web-widened segment length (3.0 m), and end diaphragm (1.2 m). The thickness of the web changes linearly from 40 cm to 60 cm. The box-girder with four cells has a width of 17.0 m at the top and 12.0 m at the bottom. Figure 1(a) shows the cross-sectional view of the mid-span of the four-cell bridge. The different positions of the web are named as shown in Figure 1(b). The outermost web of the box-girder is denoted as "side-web" (S-web). The web adjacent to the outermost web of the box-girder is denoted as "secondary side-web" (SS-web). The middle web at the centre of the cross-section is denoted as "middle-web" (M-web).

Xue [10] showed that support condition and cell number significantly affect the distribution of web shear forces. In this study, the outermost web is rotated along the centre of the web by 10°, 15°, 20°, and 25°, respectively, as shown in Figure 1(b).

The shear force distribution caused by dead load in the webs is examined under the following two conditions: (1) different support conditions (four supports, three supports, two supports), and (2) different cell number conditions (four cells and three cells).

With these two working conditions, six model series are possible, as shown in Table 1.

To examine the influence of support conditions on the shear force distribution in the webs, the analysis method is as follows: (1) Comparative analysis of the C4S2 group model, C4S3 group model, and C4S4 group model (four-cell box-girders) under different support conditions; (2) Comparative analysis of the C3S2 group model, C3S3 group model, and C3S4 group model (three-cell box-girders) under different support conditions.

Similarly, to examine the influence of cell number on the shear force distribution in the webs, the analysis method is as follows: (1) Comparative analysis of the C4S3 group model and C3S3 group model (different cell number box-girders) under three support conditions; (2) Comparative analysis of the C4S2 group model and C3S2 group model (different cell number box-girders) under two support conditions. The cross-sections of the models are shown in Figure 2.

2.2. Extraction of Web Shear Force. The mechanism of the box-girder is relatively complicated. Using the conventional theory of box-girders, the analysis results of a typical section can only be obtained under specific conditions. It is difficult to represent different support conditions and changes in structural geometry.

As shown in Figure 3(a), the cross-section of the extracted web shear force is 2/3 h distance from the support, which is the most important shear-capable check section according to the Chinese Highway Bridge Standard [13]. To study the shear force distribution law, the shear force of each web must be extracted. The range of shear force extraction for each web in this study is shown in Figure 3(b). The "Sum of Local Internal Forces" function in the Midas FEA was used to extract the shear force of each web. The specific extraction method is detailed in the literature [10].

This study focuses on the shear force distribution in webs of multicell inclined web box-girder bridges under dead loads. The applied loads are the girder self-weight and the bridge deck load. The bridge deck load is calculated at 3.5 kN/m^2 and includes a 5 cm thick concrete levelling layer and a 10 cm thick asphalt layer. The finite element model is shown in Figure 4.

3. Results of Shear Force Web Distribution

The shear force shared equally by the webs is expressed in

$$V_{\text{ave}} = \frac{V_t}{N_f}, \tag{1}$$

where V_{ave} is the nominally evenly distributed shear force of the webs, V_{t} is the full-section shear force, and N_{f} is the number of webs in the box-girder.

The dead load shear force distribution factor is defined as follows:

$$\eta_i = \frac{V_i}{V_{\text{ave}}}, \tag{2}$$

where V_{i} is the shear force value of the i-th web.

In the following analysis, the influence of the dead load shear force distribution factor is studied through the slope of the inclined web, the support conditions, and the cell number.

3.1. Effect of Slope of Inclined Web. Figure 5 shows the relationship between the dead load shear force distribution factor of the S-web, SS-web, and M-web of C4S3, C4S2, C3S3, and C3S2 and the slope of the inclined web.

In Figure 5, all dead load shear force distribution factors of the S-web are greater than 1.0; the S-web shear force values are larger than the evenly distributed shear force of the webs V_{ave}. Neglecting the uneven distribution of dead loads in the web is an unsafe design practice. In the C4S2-0° model, the dead load shear force distribution factor reaches

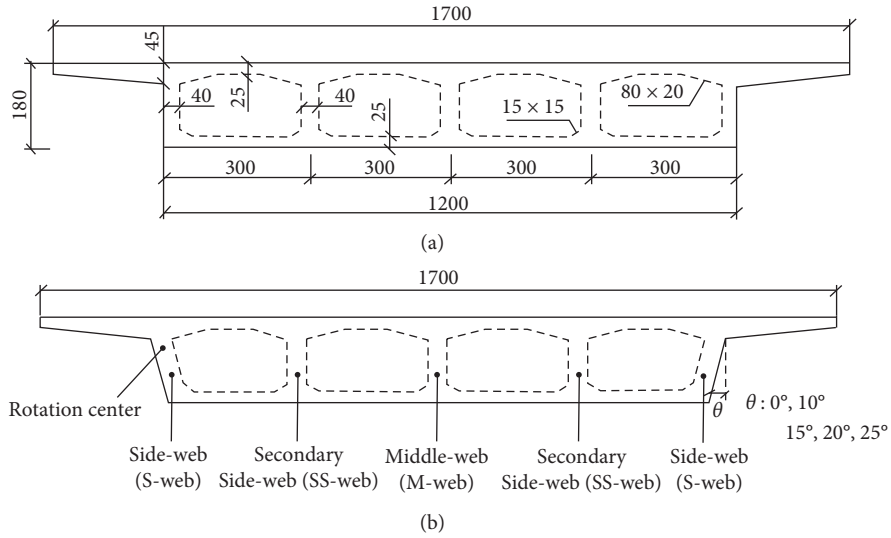

Figure 1: Basic box-girder model and rotation of the side web (unit: cm).

Table 1: Model parameters.

Model label	Slope of S-web	Number of cells	Number of supports	Description
C4S4	0°, 10°, 15°, 20°, 25°	4	4	Girder with four cells and four supports
C4S3		4	3	Girder with four cells and three supports
C4S2		4	2	Girder with four cells and two supports
C3S4		3	4	Girder with three cells and four supports
C3S3		3	3	Girder with three cells and three supports
C3S2		3	2	Girder with three cells and two supports

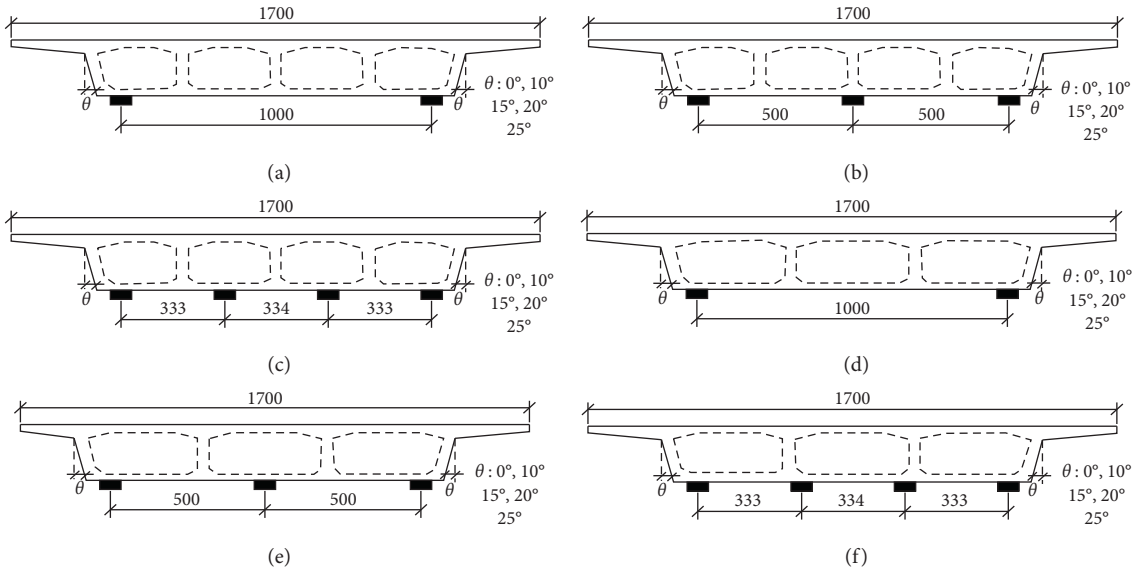

Figure 2: Shear force distribution models. (a) CAS2. (b) C4S3. (c) C4S4. (d) C3S2. (e) C3S3. (f) C3S4.

1.31. Unevenly distributed dead load shear force in the webs must be considered in the design.

From the trend line in Figure 5, as the slope of the inclined web increases, the shear force distribution of the S-web decreases, and the shear force distributions of the SS-web and M-web increase. In addition, with increasing slope of the inclined web, the dead load shear force distribution factors change a little. The dead load shear force

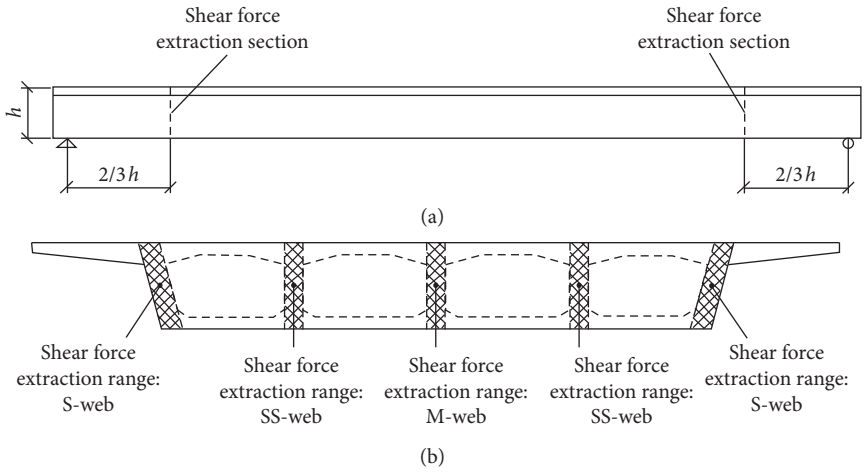

Figure 3: Shear force extraction locations for each web.

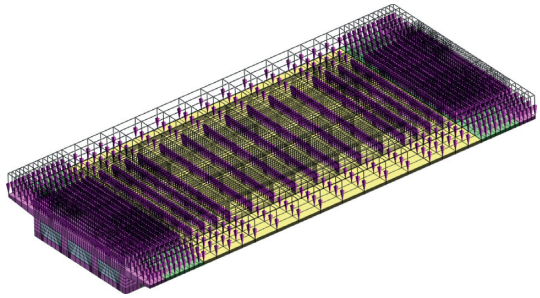

Figure 4: FEM of shear force distribution.

distribution factors of C4S3-0° and C4S3-25° decrease from 1.17 to 1.11, a difference of 5.13%. Other model series exhibit a similar trend, indicating that the slope of the inclined web has a slight effect on the dead load shear force distribution factors.

3.2. Effect of Support Condition. C4S4, C4S3, and C4S2 have the same cross-section; they have four cells with four supports, three supports, and two supports, respectively. Similarly, the cross-sections of C3S4, C3S3, and C3S2 are the same; they have three cells with four supports, three supports, and two supports, respectively. Through these two sets of model sequences, the corresponding impacts of supports on the dead load shear force distribution factors are compared and analysed.

Figure 6 compares the dead load shear force distribution factors of the S-web for the two box-girders under four supports, three supports, and two supports, respectively.

From Figure 6, the impact of supports on the dead load shear force distribution factors of the S-web is obvious: (1) For models with four cells, the dead load shear force distribution factors of the S-web with two supports increased by 10.0–10.8%, compared to those of the S-web with three supports, and increased by 14.5–15.5%, compared to those of the S-web with four supports; (2) For models with three cells, the dead load shear force distribution factors of the S-web with two supports increased by 6.8–7.8% and 8.2–8.7% compared to those of the S-web with three supports and four supports, respectively. This is critical information in bridge design.

With an increasing number of supports, the support reaction force acting on the girder decreases, and the shear force in the web tends to be evenly distributed. And this is more powerful for bridge design.

3.3. Effect of Cell Number. In Figure 7, the dead load shear force distribution factors of the S-web in box-girders with different cell numbers under the same support conditions are compared. The cell number has a significant influence on the dead load shear force distribution factors. When the cell number decreased from four cells to three cells, the number of webs decreased, the dead load shear force distribution factors decreased, and the shear force distribution became more uniform.

(1) With two supports, the dead load shear force distribution factors with three cells are reduced by 12.2–13.4% compared to those with four cells.

(2) With three supports, the dead load shear force distribution factors with three cells are reduced by 8.5–10.4% compared to those with four cells.

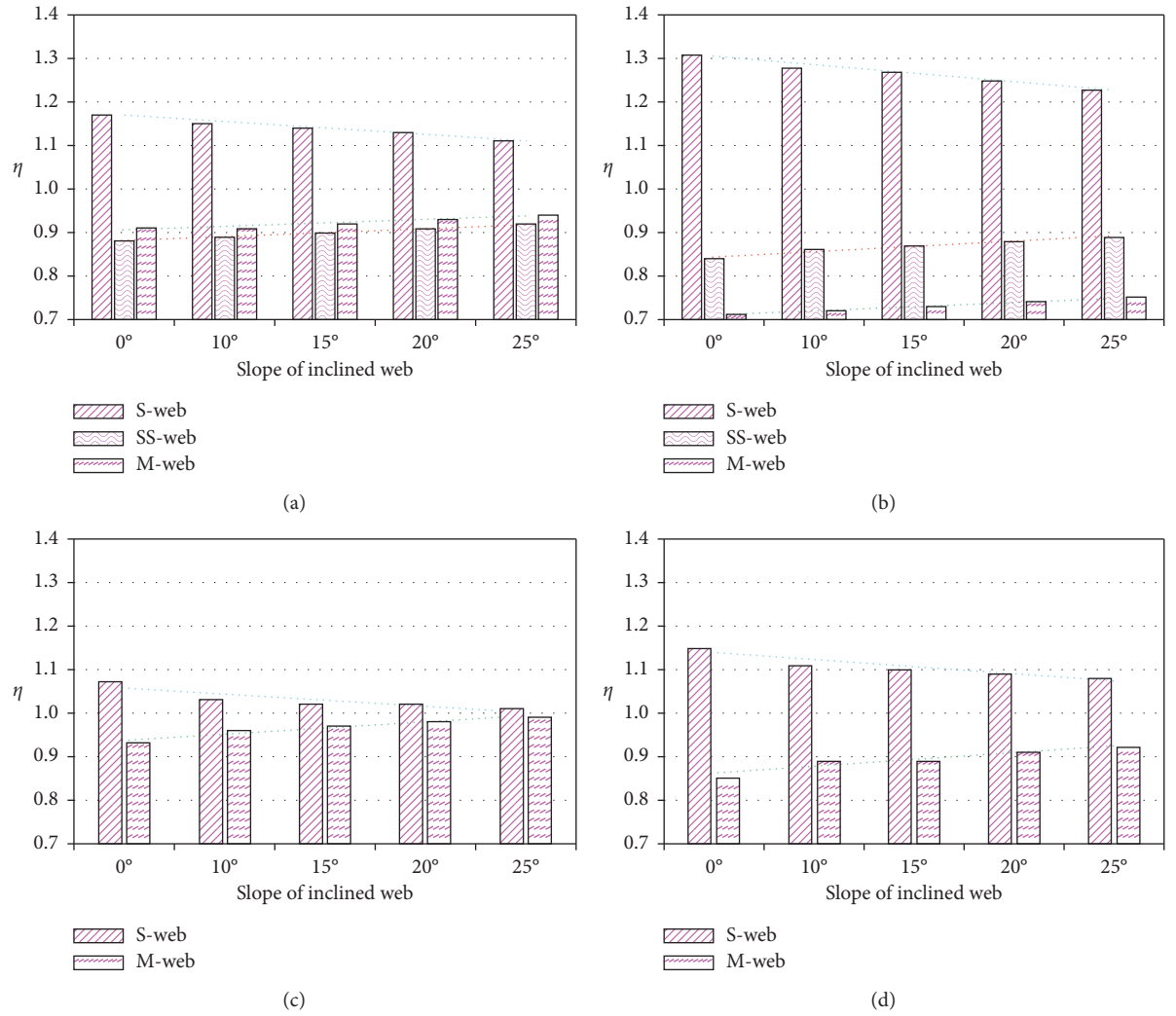

Figure 5: Effect of slope of inclined web. (a) C4S3. (b) C4S2. (c) C3S3. (d) C3S2.

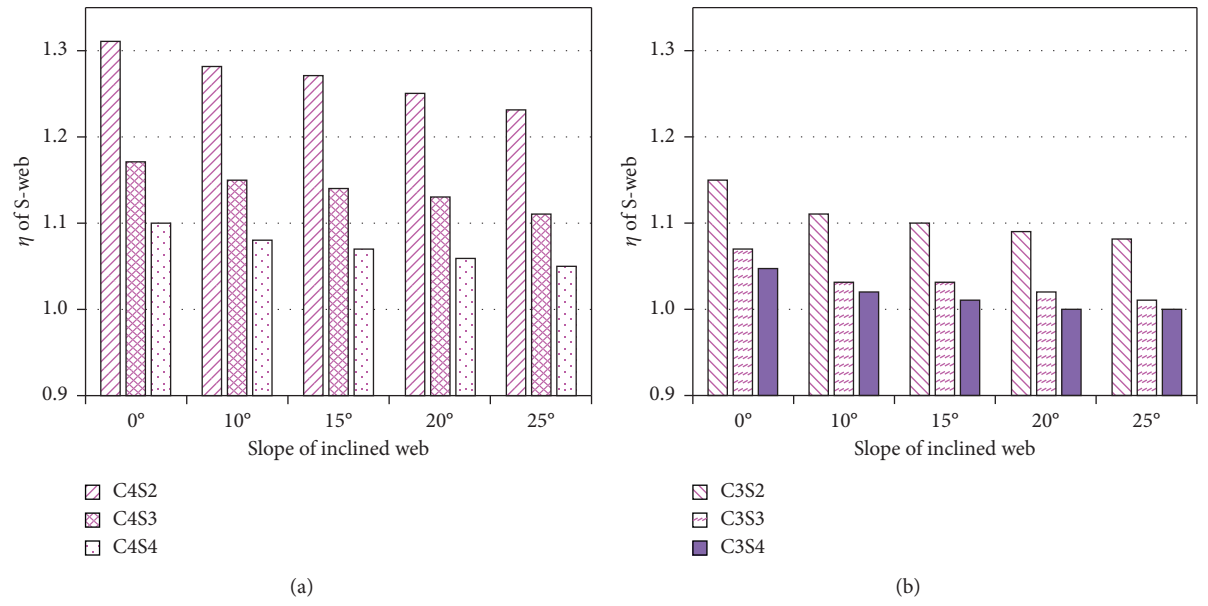

Figure 6: Effect of support condition. (a) C4S2, C4S3, and C4S4. (b) C3S2, C3S3, and C3S4.

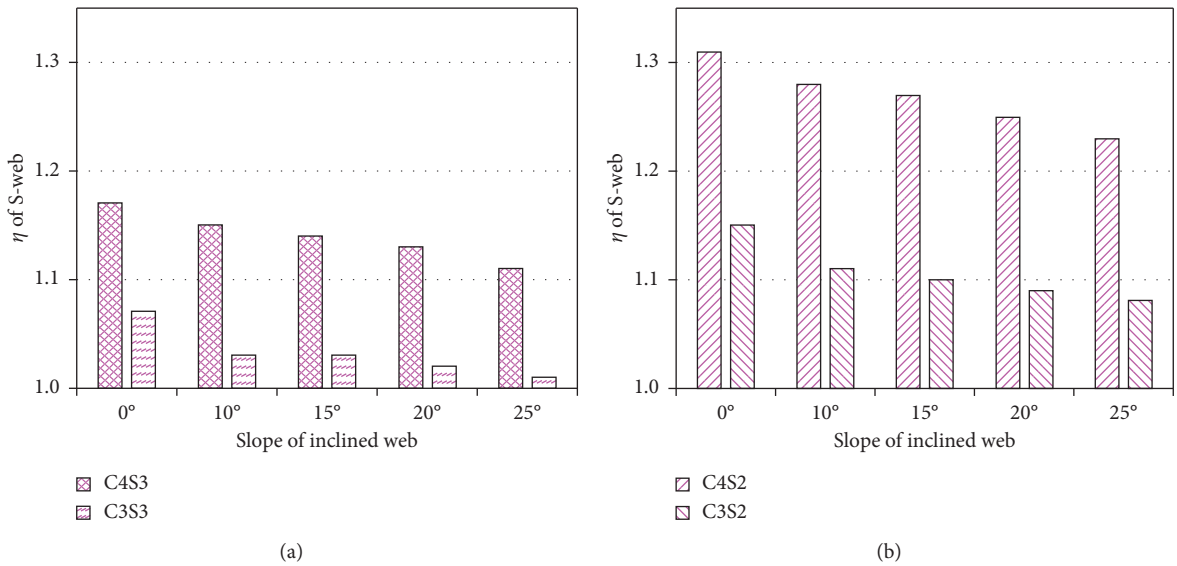

Figure 7: Effect of cell number. (a) C4S3 and C3S3. (b) C4S2 and C3S2.

4. Shear Force Web Redistribution in the Cracked State

Section 3 discusses the distribution law of the dead load shear force distribution in webs of a multicell inclined web box-girder bridge in an elastic state. This section focuses on shear force web redistribution in the cracked state.

4.1. Nonlinear Finite Element Model. C4S2 was selected as the nonlinear calculation model. To simplify the calculation, the thickness of the web was set uniformly to 60 cm.

The box-girder stirrups have a diameter of 12 mm and a spacing of 10 cm; the diameters of the longitudinal reinforcements of the bottom plate and top plate are 28 mm and 16 mm, respectively. Using displacement loading, to avoid stress concentration in the loading position and support position, elastic cushion blocks are used. The distance between the loading position and the support position is h, the elastic modulus is 2×10^5 MPa, and Poisson's ratio is set to 0.2 to improve calculation efficiency. The end diaphragm is set as an elastic material; the other materials are nonlinear, as shown in Figure 8.

For the compression and tension of concrete, a parabolic compression model and a linear softening tension model [10, 12] of the total strain crack model are used, respectively. The strength grade of the concrete is C40. The von Mises model is used for the reinforcement. The stirrups and longitudinal steel bars are of HPB300 and HRB400 grades, and the corresponding yield strengths in the calculation are 300 MPa and 400 MPa, respectively. The slip between the rebar elements and the parent elements is not considered in the calculation. The strain of the rebar element is calculated by the displacement of the parent element.

4.2. Results of Shear Force Web Redistribution

(1) Load-displacement curves and cracks

The vertical displacement of each web in the span is extracted under load, as shown in Figure 9.

In Figure 9, the difference between the three web load-displacement curves is small. Before the load reaches point P1, the box-girder is in the elastic phase *a-b*. As the load increases to load point *P*1 (*P*1 = 10200 kN), the S-web cracks first, as shown in Figures 10(a) and 11(a). When the load increases by 255 kN, reaching 10455 kN (*P*2 load point), the SS-web and M-web crack successively, and the cracks of S-web further develop, as shown in Figures 10(b) and 11(b). When load points *P*3 and *P*4 are reached, the longitudinal steel bar yields; even if the load slightly increases, the crack develops sharply to the upper- and mid-span of the girder, as shown in Figures 10(c) and 10(d). During the subsequent loading process, the strengthening phase *c-d* is entered, and the bearing capacity continuously increases until failure.

(2) Shear force web redistribution in the loading process

Midas FEA can still use the "Sum of Local Internal Forces" function to extract the shear force of each web in the concrete cracking stage, and the shear force web redistribution in the cracking stage can be analysed. The cross-section shear force is extracted at each load Step $2/3\,h$ away from the support (Figure 3(a)); the displacement is extracted in the middle span. After extracting the shear forces of S-web, SS-web, and M-web, the dead load shear force distribution factor is calculated, as shown in Figure 12.

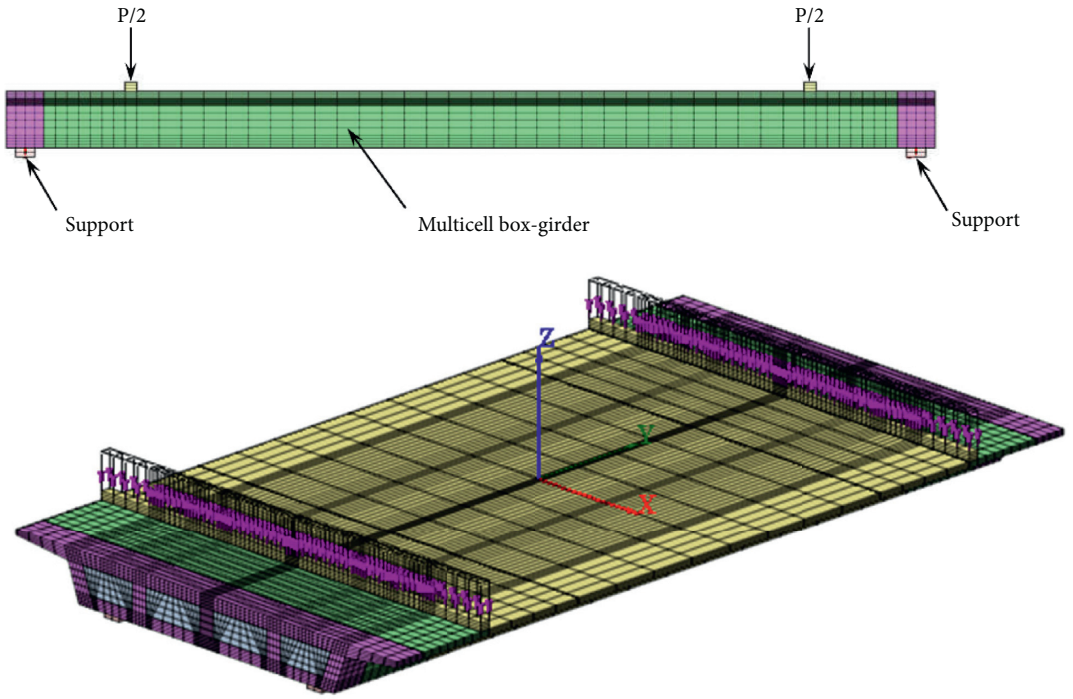

Figure 8: Nonlinear finite element model.

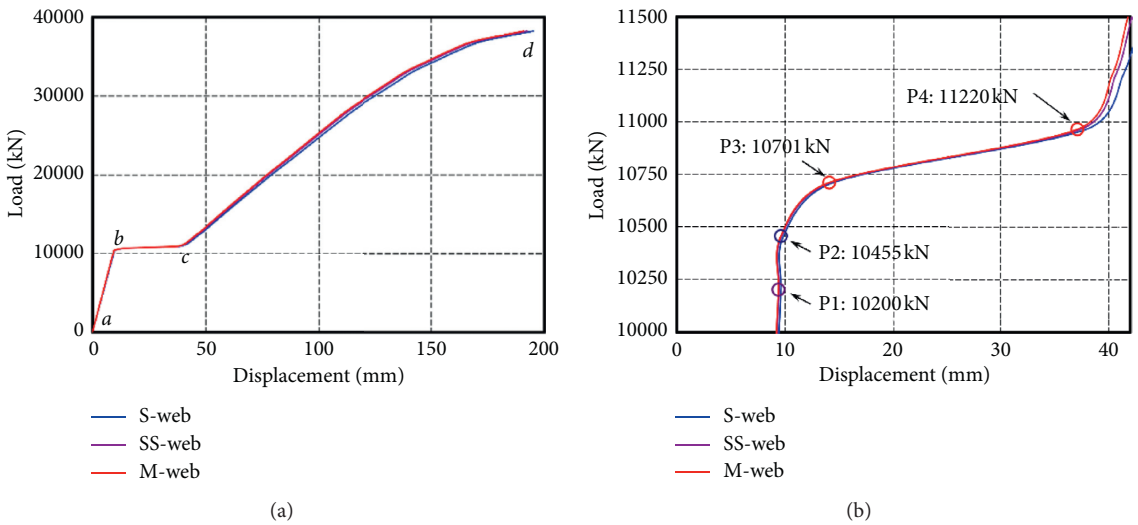

Figure 9: Load-displacement curves.

From Figure 12:

(1) In the elastic phase, the dead load shear force distribution factor remains the same even if the external load changes. The dead load shear force distribution factor of the S-web is greater than 1.0. The shear force distribution factors for S-web, SS-web, and M-web are 1.27, 0.83, and 0.79, respectively.

(2) After loading to point P1 (10200 kN), S-web cracked first. After the fluctuation of the local data, the dead load shear force distribution factor of the S-web increased to 1.41 (P = 10965). As the load continued to increase, the dead load shear force distribution factor of the S-web decreased to 1.31 (P = 12750). The SS-web and M-web dead load shear force distribution factors decreased with increasing S-web dead load shear force distribution factor and increased with decreasing S-web dead load shear force distribution factor. A redistribution of shear forces occurred between the webs.

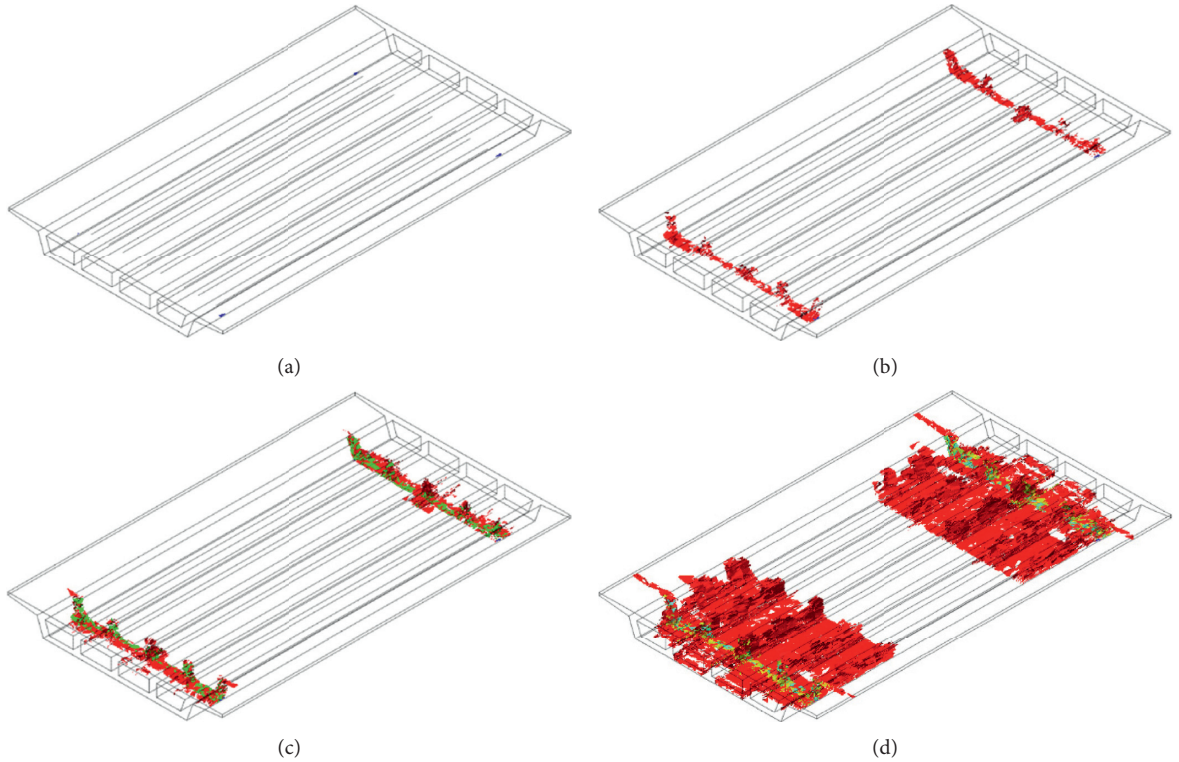

Figure 10: Crack development of box-girder. (a) $P1 = 10200$ kN. (b) $P2 = 10455$ kN. (c) $P3 = 10701$ kN. (d) $P4 = 10956$ kN.

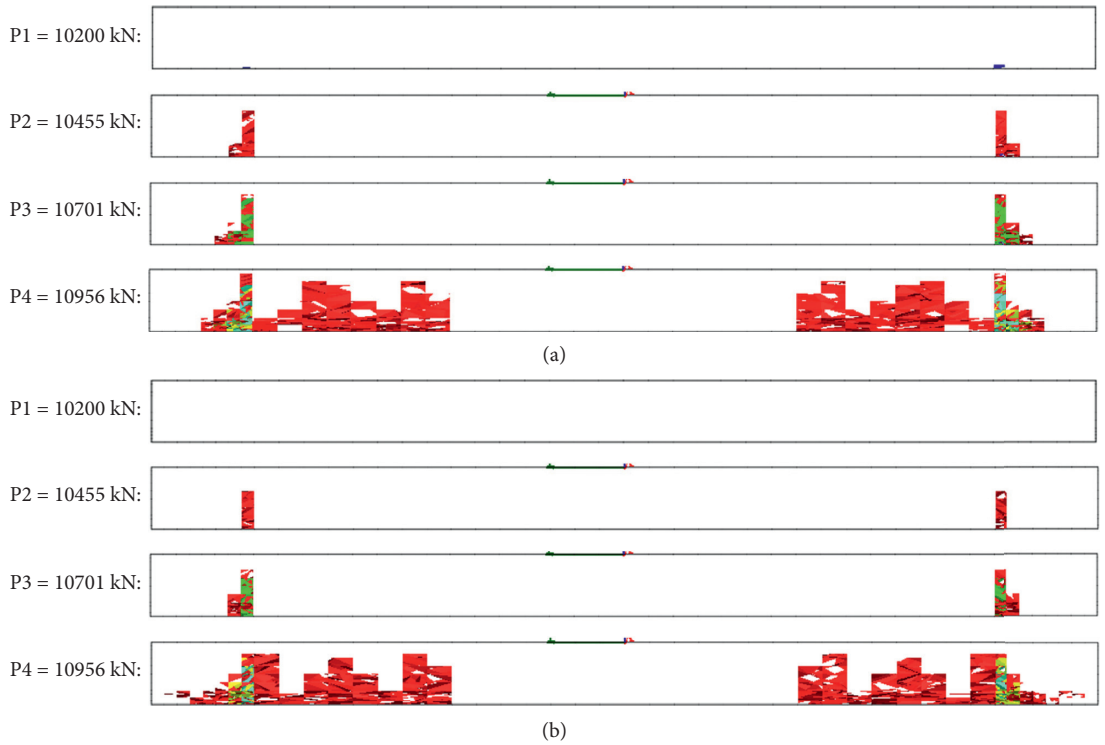

Figure 11: Continued.

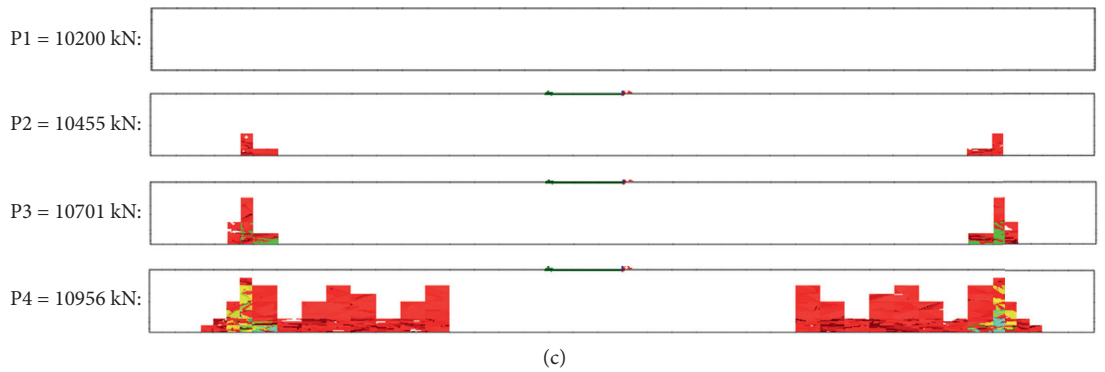

Figure 11: Longitudinal section of web crack. (a) S-web. (b) SS-web. (c) M-web.

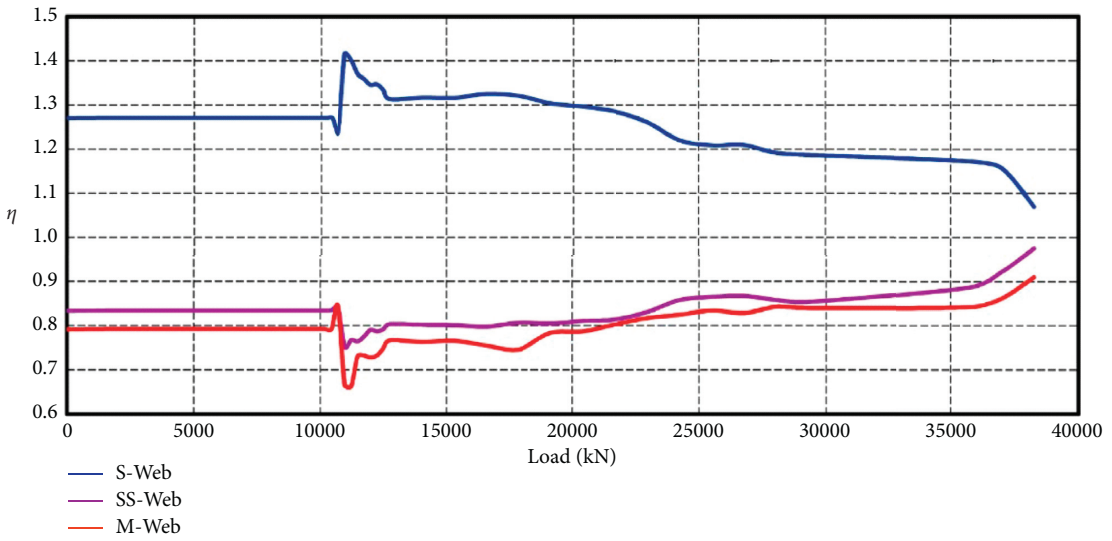

Figure 12: Shear force web redistribution in loading process.

5. Conclusions

To investigate the influence of shear force distribution in the webs of multicell inclined web box-girder bridges under a dead load, a 3D finite element model was adopted to extract the shear force of each web via the "Sum of Local Internal Force" method. The effects of different web slopes, support conditions, and cell numbers on the dead load shear force distribution factor are summarised; the main conclusions are as follows:

(1) The S-web shear force under dead load is generally greater than 1.0, which is unsafe in the shear design of bridges. Shear failure is brittle or quasi-brittle. The shear force of the S-web under dead load is greater than the average shear force and should be considered. The dead load shear force distribution factor can be used to express the degree to which the web bears dead load shear force. The concept is clear, which is beneficial to bridge design and assessment of bridge shear safety.

(2) The cell number has a greater impact on the dead load shear force distribution factor than the support condition; the impact of these two factors should be fully considered when designing the box-girder. As the slope of the S-web increases, the dead load shear force distribution factor of the S-web gradually decreases, and the dead load shear force distribution factor of the middle webs increases. In addition, the slope of the S-web has a slight effect on the shear distribution of the webs.

(3) In the elastic phase, the dead load shear force distribution factor remains unchanged. A redistribution of shear forces occurs between the webs in the elastoplastic phase, but the S-web dead load shear force distribution factor is always greater than 1.0.

Data Availability

The data used to support the findings of this study are available from the corresponding author upon request.

Conflicts of Interest

The authors declare that they have no conflicts of interest regarding the publication of this article.

Acknowledgments

This research was funded by the Scientific Research Project of Educational Department of Liaoning Province (LNZD202005) and Higher Education Innovative Talent Support Plan of Liaoning (LR2019057).

References

[1] S. T. Chang, "Prestress influence on shear-lag effect in continuous box-girder bridge," *Journal of Structural Engineering*, vol. 118, no. 11, pp. 3113–3121, 1992.

[2] M. W. Sarwar and T. Ishihara, "Numerical study on suppression of vortex-induced vibrations of box girder bridge section by aerodynamic countermeasures," *Journal of Wind Engineering & Industrial Aerodynamics*, vol. 98, no. 12, pp. 701–711, 2010.

[3] P. Mondal and J. T. Dewolf, "Development of computer-based system for the temperature monitoring of a post-tensioned segmental concrete box-girder bridge," *Computer-Aided Civil and Infrastructure Engineering*, vol. 22, no. 1, pp. 65–77, 2007.

[4] Q. J. Wen, "Long-term effect analysis of prestressed concrete box-girder bridge widening," *Construction & Building Materials*, vol. 25, no. 4, pp. 1580–1586, 2011.

[5] C. K. Choi, K. Kim, and H.-S Hong, "Spline finite strip analysis of prestressed concrete box-girder bridges," *Engineering Structures*, vol. 24, no. 12, pp. 1575–1586, 2002.

[6] S. T. Song, Y. H. Chai, and S. E. Hida, "Live-load distribution factors for concrete box-girder bridges," *Journal of Bridge Engineering*, vol. 8, no. 5, pp. 273–280, 2003.

[7] N. Suksawang, H. Nassif, and D. Su, "Verification of shear live-load distribution factor equations for I-girder bridges," *Ksce Journal of Civil Engineering*, vol. 17, no. 3, pp. 550–555, 2013.

[8] B. Z. Dymond, *Shear Distribution in Prestressed Concrete Girder Bridges*, University of Minnesota, Minneapolis, MN, USA, 2015.

[9] W. Choi, I. Mohseni, J. Park, and J. Kang, "Development of live load distribution factor equation for concrete multicell box-girder bridges under vehicle loading," *International Journal of Concrete Structures and Materials*, vol. 13, no. 22, pp. 1–14, 2019.

[10] X. Xue, "Numerical investigation of distribution laws of shear force in box girder webs," *Advances in Materials Science and Engineering*, vol. 2019, pp. 1–14, Article ID 9865989, 2019.

[11] X. Xue, J. Zhou, X. Hua, and H. Li, "Analysis of the generating and influencing factors of vertical cracking in abutments during construction," *Advances in Materials Science and Engineering*, vol. 2018, pp. 1–13, Article ID 1907360, 2018.

[12] Y. Huang, G. Liua, S. Huang, R. Rao, and C. Hu, "Experimental and finite element investigations on the temperature field of a massive bridge pier caused by the hydration heat of concrete," *Construction and Building Materials*, vol. 192, pp. 240–252, 2018.

[13] Ministry of Transport of the People's Republic of China, *JTG 3362–2018, Specifications for Design of Highway Reinforced Concrete and Prestressed Concrete Bridges and Culverts*, Ministry of Transport of the People's Republic of China, Beijing, China, 2018.